Defence Science Journal, Vol. 75, No. 3, May 2025, pp. 371-378, DOI : 10.14429/dsj.19742

Design of Metamaterial Based Circularly Polarized Antenna for Anti-Drone Applications

Sukhdas Ahirwar[#,*], Amara Prakasa Rao[$] and Mada Chakravarthy[#]

[#]*DRDO-Defence Electronics Research Laboratory (DLRL), Hyderabad - 500 005, India*
[$]*Deparment of ECE, National Institute of Technology (NIT), Warangal - 506 004, India*
[*]*E-mail: ahirwar.s.dlrl@gov.in*

ABSTRACT

This paper presents the design and realization of a circularly polarized antenna for anti-drone applications. A broadband Archimedean spiral antenna is designed as a radiating element for circular polarization. A metamaterial ground plane is designed and used as a reflector for the spiral antenna. The extraordinary properties of metamaterial ground plane are used to transform the radiating element into high-gain, low-profile antenna. The unit cell for metamaterial ground plane is derived from the Mushroom-like Electromagnetic Band Gap (EBG) cell. The frequency band of operation of this cell is more than its parent cell. The achieved bandwidth for this modified cell is 117.6 %. The working frequency range for the proposed antenna is 0.8-3 GHz. This frequency band of operation covers 900 MHz, 1.1 GHz -1.7 GHz and 2.4 GHz frequency bands being used in drone technology. Antenna gain varies from 5 dBic to 8.5 dBic over the band. The impedance, radiation patterns and, 3 dB on and off axes ratio bandwidths are 115.8 %. The parametric studies are carried out to optimize the electrical performances of EBG cell, spiral antenna, and EBG ground plane. The spiral antenna is backed by a metamaterial reflector. The simulated/ measured results are presented. The antenna height is reduced by 68 % compared to conventional cavity-backed spiral antennas.

Keywords: Antenna; Anti-drone; EBG; CS-UCEBG; Spiral

NOMENCLATURE

a	: Periodicity of EBG cell
b	: Width of EBG patch
g	: Gap between EBG patches
h	: Substrate height
L_s	: Slot length
N_s	: No. of turns of spiral
r	: Radius of spiral L_s Slot length
W_s	: Slot width
λ_L	: Wave-length at lower frequency of operation

1. INTRODUCTION

Electromagnetic band-gap (EBG) structures are artificially engineered structures known as metamaterials. These materials exhibit certain electromagnetic properties which are not available in natural materials. These materials exhibit a frequency band gap and the surface waves are suppressed in this frequency band. This property of the materials is useful in the electrical performance improvement of planar antennas. These structures also provide high impedance in their frequency range of operation. Such type of surfaces also reflects the incident waves in same phase. Due to this in-phase reflection property of these structures, they are known as Perfect Magnetic Conductors (PMC) or Artificial Magnetic Conductors (AMC). This property of structures can be used to place radiating antenna element very close to the EBG/AMC ground plane/ reflector. Mushroom-like[1] EBG structure is the most important 2D EBG structure. The basic EBG cell of this structure consists of a metallic patch on metalized (grounded) substrate. At the center, this patch is shorted electrically to ground through a metallic post known as via. This cell is modified in form of shifting the via from the center along the x or y-axes to have polarization- dependent characteristics[2]. In-phase reflection bandwidth of the cell is enhanced by shifting the via diagonally from the center of the cell[3]. In this proposed design, the 4 numbers of vias are used at 4 corners of the cell to have wider bandwidth. The use of 4 vias, maintains the symmetry of the cell required for circularly polarized antennas. The drones small are Unmanned Aerial Vehicles (UAV) operated by a pilot remotely. With inception of drone technology, the drone industry's expansion is increasing rapidly. Today these flying machines are being utilized for aerial photography, disaster management, search and rescue operations, law enforcement, weather forecasting, goods delivery[4] etc. to name a few. They are now a part of armed forces operations[5]. Over time the drones are being used for the malicious and unlawful activities and these activities have been increased manifold. Such incidences related to such types of activities are being reported worldwide[6].

The anti-drone system consists of detection, interception, classification/ identification, and mitigation of drones.

Received : 02 January 2024, Revised : 21 March 2025
Accepted : 24 March 2025, Online published : 08 May 2025

To identify the drones, there are 4 basic parameters-radio frequency sensors, acoustics sensors, optical sensors, and radar. With RF analyzers, the antennas are used to receive radio waves and the RF spectrum is analyzed. This analysis is required to detect the radio communication between drone and its controller (pilot). This communication happens at various frequency bands starting from 433 MHz to 5.8 GHz. These frequency sub-bands are 433 MHz, 900 MHz, 1.1-1.7 GHz, 2.4 GHz, and 5.8 GHz frequency bands. The particular frequency band is used selectively based on range to be covered, required data rate and polarization. For drone detection, the circularly polarized antennas are preferred for better handling of polarization mismatch in the link. Moreover, to intercept the GPS signals in GPS controlled drones the circularly polarized antennas are needed. The axial mode helical antennas are used generally for this purpose. The helical antennas have lesser bandwidth and hence separate antennas are required in different frequency bands. Beam width for these antennas is lesser and hence less spatial coverage in desired direction compared to spiral antennas[7]. These antennas are also having more height. The spiral antenna with reasonably good gain can be an option against helical antennas to have low-profile, broad bandwidth and broad beam width antennas. In this paper, such type of broadband antenna with EBG reflector is presented. The paper is organized as follows-

- Design, realization and performance evaluation of metamaterial ground plane
- Design, realization and performance evaluation of spiral antenna and
- Design, realization and performance evaluation of spiral antenna with metamaterial ground plane.

2.1 DESIGN AND PERFORMANCE EVALUATION OF METAMATERIAL GROUND PLANE

The smallest unit of metamaterial ground plane is known as the unit cell. The electrical characteristics of this cell decide the performance of ground plane. In this proposed design, a mushroom-like EBG cell is used to design a comparatively broadband unit cell. The mushroom-like EBG cell consists of a square metallic patch on the grounded dielectric substrate. The patch width is denoted with W = b and periodicity of this patch is denoted by a = W+g, where g is the gap between cells. This patch is shorted to metallic ground plane at center through a post known as via. The other design parameters for this cell are via diameter (2r), substrate height (h), and dielectric constant of substrate (ϵ_r).

At lower frequency of operation, the required cell dimensions are b = 0.12λ, g = 0.02λ, d = 0.05λ, where λ is the wavelength corresponding to frequency of operation. Based on EBG ground plane size requirement for the antenna, the mushroom-like cell is modeled in an FDTD based simulation tool. The FR4 sheet of height 1.6 mm, ϵ_r = 4.4 and tanδ = 0.02 is used as a substrate in this design. The patch width W = b = 22 mm is the optimized width for better electrical performance in the frequency band of operation. Electrically, this cell size is 0.12λ at 1.6 GHz. The performance of the cell is evaluated by evaluating the S-parameters of the EBG ground plane. This ground plane consists of periodically arranged EBG cells in 2D. In[2] it was studied that the shifting the via from center in the x or y-direction the polarization dependent EBG cell is obtained. The concept of via shifting was used for better operational bandwidth without disturbing the polarization characteristics. The basic mushroom-like EBG cell is modified by inserting 4 vias in place of single central via. The 4 vias are used to maintain the cell symmetry along the x and y-axes.

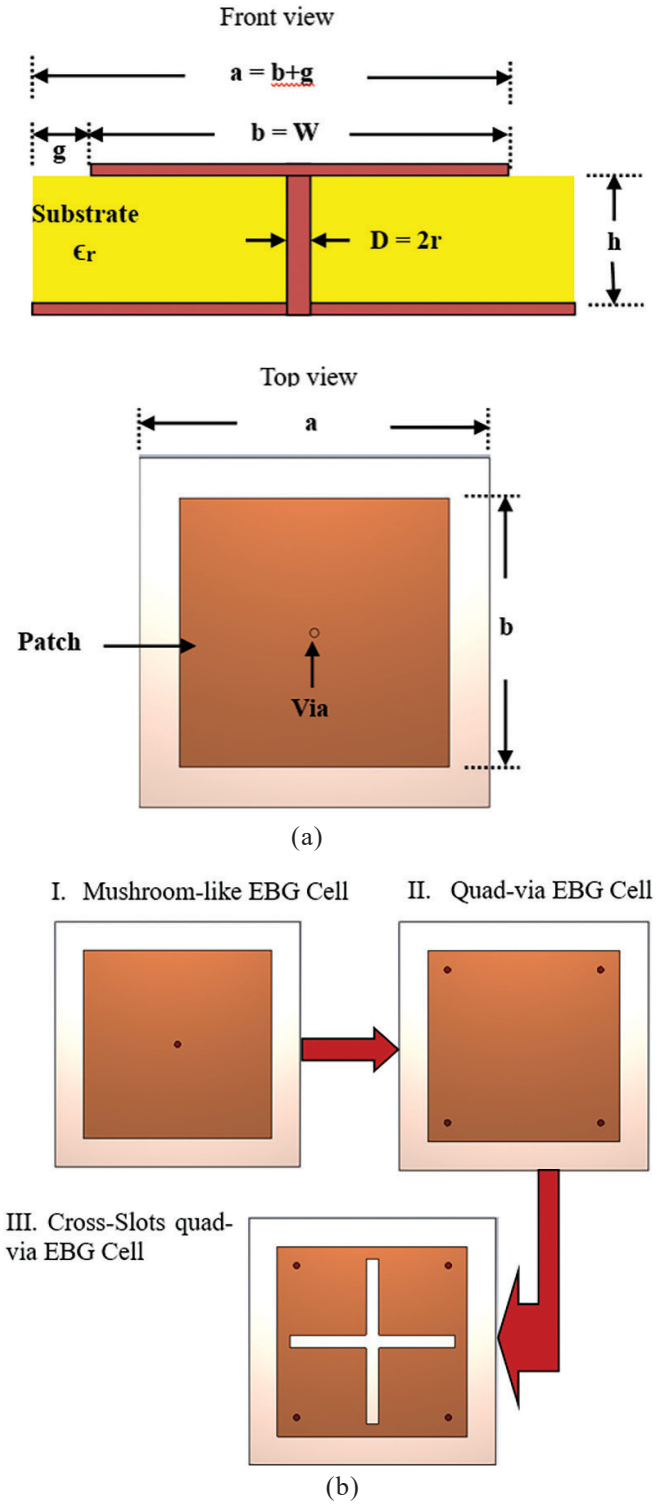

Figure 1. EBG cell details and development stages; (a) Constructional details of Mushroom-like EBG cell; and (b) Transformation of Mushroom-like EBG cell into cross-slots quad-via EBG cell.

S-parameters are studied by shifting these vias diagonally from center (0, 0) to (d, d) and bandwidth improvement is achieved.

For further improvement, the cross-slots are introduced in the patch. This configuration provides the maximum bandwidth. The constructional details of mushroom-like EBG cell and its transformation from mushroom-like EBG cell to Cross-slots quad-via EBG cell are shown in Fig. 1. All the optimized dimensions for this cell are given in Table 1.

Table 1. Details of parameters of proposed EBG cell

Parameter	Expression	Actual value (mm)
Patch width (W=b)	0.12λ	22
Gap (g)	0.2b	4.4
Periodicity (a)	b+g	26.4
Via dia.(D)	----	0.5
Via. Position (d, d)	(0.4W, 0.4W)	(8.8 , 8.8)
Substrate ht. (h_s)	----	1.6
Slot length (L_s)	----	20
Slot width (W_s)	----	1

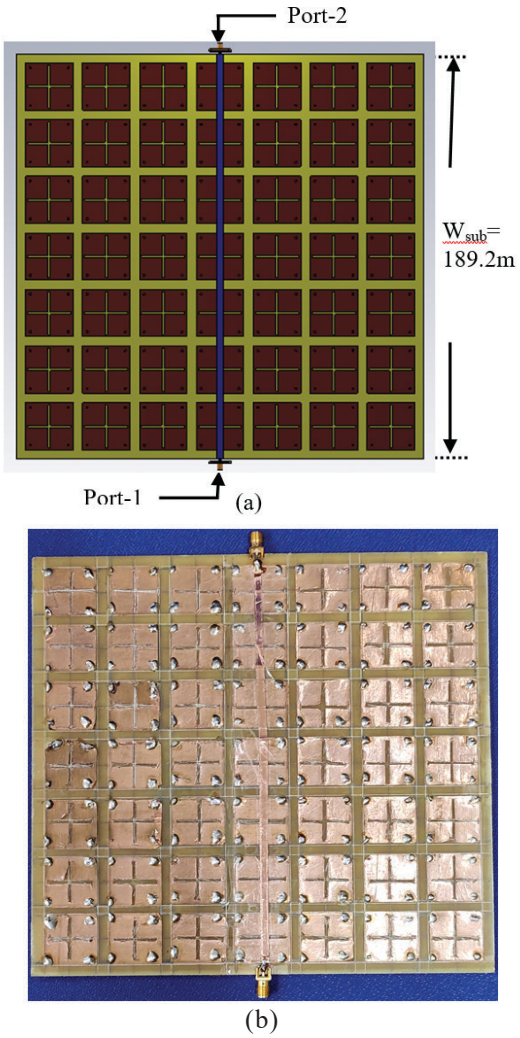

Figure 2. Cross-slot quad-via EBG ground plane (a) Simulation model; and (b) Photograph.

For performance comparison of these cells, the EBG ground planes consisting of 7 x 7 cells are modeled. The required size of the substrate to accommodate these cells is 189.2 mm x 189.2 mm. A50Ω microstrip line is modeled over the EBG ground plane for two-port S-parameter measurement. The spacing between line and EBG structure is kept at 0.1 mm. The EBG ground plane model consisting of proposed EBG cells and photograph of this ground plane are shown in Fig. 2.

The proposed ground plane was simulated for its S-parameters at different stages. These stages are created by shifting the vias as function of via spacing (d, d) from the center. Theoretically, in the frequency band of operation, the value of S_{11} should be near zero dB and the value of S_{21} should be below -10 dB. These values of S-parameters show the electromagnetic band gap of EBG ground plane. The overlay of simulated S_{21} plots for different stages of the cell is shown in Fig.3 (a). From Fig.3 (a), it can be seen that the higher cut-off frequencies are similar for all the cell configurations. The lower frequency of operation for mushroom-like EBG cell is 1.9 GHz, showing the shift in lower frequency of operation

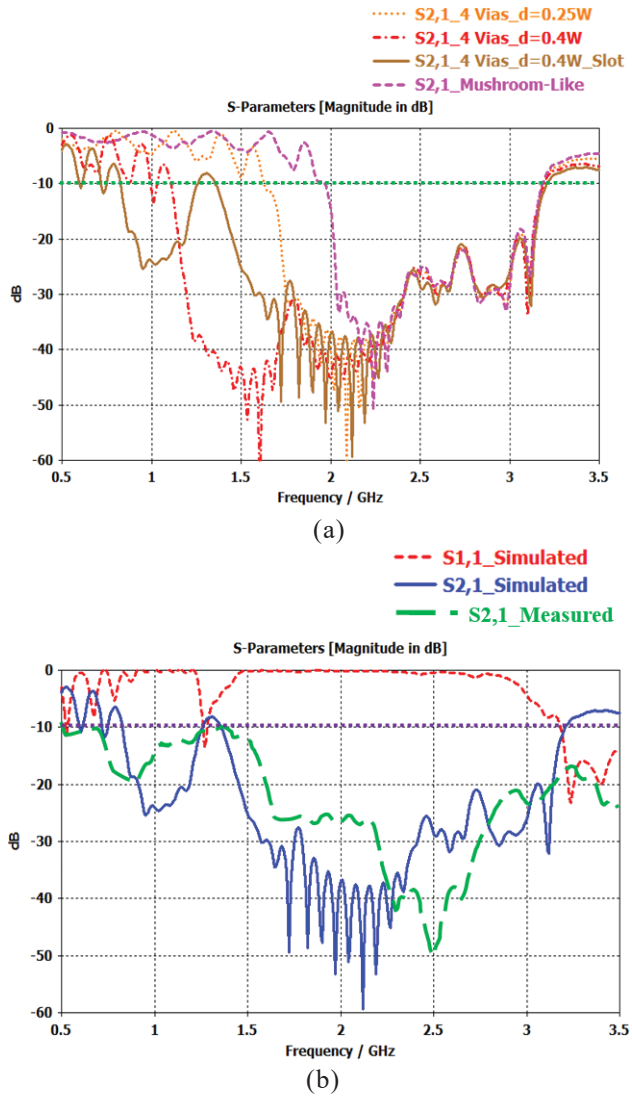

Figure 3. Comparison of S-parameters of proposed EBG ground plane (a) S21 parameters for different cell configurations; and (b) S-parameters for final cell configuration.

against the design frequency of 1.6 GHz. With quad-via cells, an improvement in lower frequency of operation is observed by shifting the vias diagonally. This improvement is better for more value of d. The optimum value for d is 0.4 W. With further increase in d degrades the cell performance. Finally, for optimized value of d the cross-slot is created in the cell and studied for cell performance. With this cross-slot, further improvement in bandwidth is achieved. The slot length (L_s) and slot width (W_s) are taken as parameters to study the electrical response of the cell. It is observed that the performance is highly dependent on slot length but it is less sensitive to slot width. The bandwidth for these stages is shown in Table 2. The overlay of simulated S-parameters (S_{11}, S_{21}) and measured S_{21} plots for ground plane of quad-via cross-slot EBG cell for optimized dimensions is shown in Fig. 3(b). As evident from Fig. 3(b), the operational bandwidth for this EBG ground plane is 0.8-3 GHz with a small deviation in S-parameters at a spot frequency of 1.3 GHz.

Table 2. Bandwidths of the EBG cell at different stages

EBG Cell configuration	f_L (GHz)	f_H (GHz)	BW (%)
Mushroom-like	1.97	3.2	47.6
Quad-via, d=0.25W	1.6	3.2	66.7
Quad-via, d=0.4W	1.1	3.2	97.7
Quad-via, d=0.4W with cross-slots	0.83	3.2	117.6

2.2 Design, Realisation and Performance Evaluation of Spiral Antenna

The Archimedean spiral antennas are wideband[8]. When antennas are defined in terms angles, they are wide-band antennas and known as frequency-independent antennas. The two arms of the spiral are flared out as a function of angle (Φ). Radius of spiral arm is defined as

$$r = a\varphi + r_1 \quad (1)$$

Since the other arm of spiral is angularly displaced by 180º (π rad.), the radius for this second arm is defined as

$$r = a(\varphi - \pi) + r_1 \quad (2)$$

where, r_1 = initial radius of spiral, r = instantaneous radius of spiral, and a=constant, controls the flaring rate of spiral.

The low-frequency response of spiral is decided by the maximum radius, $r = r_2$, and high frequency response is governed by minimum radius, $r = r_1$. In terms of these radii the low and high frequencies of operation are defined as follows-

$$f_{LOW} = c/(2\pi r_2) \quad (3)$$

$$f_{HIGH} = c/(2\pi r_1) \quad (4)$$

where, c is velocity of EM wave.

If W= width of spiral conductor, S= Spacing between two adjacent conductors and N= Number of turns of spiral then these parameters are related as follows-

$$W = [(r_2 - r_1)/2N] - S \quad (5)$$

For complimentary structures, S= W and

$$S = W = (r_2 - r_1)/4N \quad (6)$$

According to Babinet's principle, the characteristics impedance of spiral antenna with its complementary is 188.5 Ω. In practical antennas this value may range 120 to 150 Ω.

In tightly wound spirals, the compact size can be achieved at the cost of antenna gain. As these spirals have more loss resistance. On the other hand, the better gain can be achieved with loosely wound spirals. A loosely wound spiral is designed for better gain in this proposed design. The spiral antenna

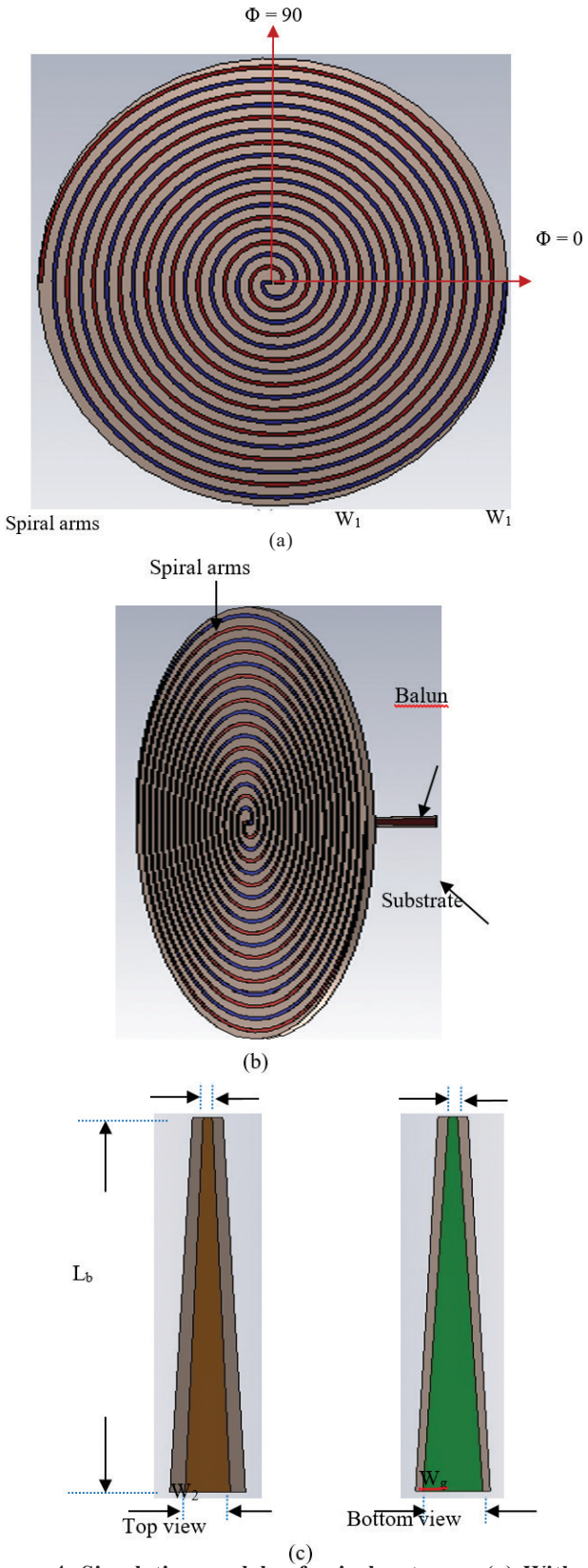

Figure 4. Simulation models of spiral antenna; (a) Without balun; (b) With balun; and (c) Balun details.

is modeled on an FR4 substrate having height of 1.6 mm, ϵ_r = 4.4 and loss tangent = 0.02. This spiral is simulated with a fixed port impedance of 140Ω. The antenna is optimized for several turns concerning impedance matching, radiation patterns, and axial ratio over the band. Now for same number of turns, a tapered balun is designed, integrated with spiral and simulated for above parameters. The simulation models of the spiral antenna without and with balun are shown in Fig. 4. The optimized design parameters of the spiral antenna with balun are shown in Table 3.

Table 3. Detail of parameters of spiral antenna with balun

Parameter	Value (mm)
Width of spiral conductor (W_s)	1.5
Gap between Spiral conductors (G_s)	4.0
Initial radius of spiral (r_1)	3.0
Maximum radius of spiral (r_2)	93.75
No. of turns (N_s)	8
Substrate Radius	94
Balun length (L_b)	40
Minimum strip width (W_1)	0.6
Maximum strip width (W_2)	1.5
Maximum ground plane strip width (W_g)	4.0

2.3 Performance Evaluation of Spiral Antenna Integrated with Metamaterial Ground Plane

The spiral antenna is backed with the metamaterial ground plane. This ground plane is used as a reflector for the spiral. This integrated antenna is simulated for all electrical parameters. This simulation model and photograph of the antenna with return loss measurement setup are shown in Fig. 5.

The spacing (S) between spiral and reflector is taken as a parameter and a parametric study is carried out. It is observed that for S=35 mm, all the electrical parameters are satisfactory. The overlay of return loss at different stages and measured return loss for proposed antenna are shown in Fig. 6.

As can be seen from the return loss plots, return loss for the spiral antenna with constant port impedance of 140Ω is ≥10 dB above 0.75 GHz. For other two cases the 10 dB return loss bandwidth starts from 0.6 GHz. The magnitude of S_{11} is ≥10 dB for all the cases. The circular polarization capability of the antennas is measured in terms of axial ratio. As a function of spacing, the boresight axial ratio (AR) is plotted over the frequency band. It is observed that for smaller spacing, the on-axis axial ration is better at higher frequencies. At lower frequencies, this AR is better for larger spacing. The 3 dB axial ratio bandwidth is 0.8-3 GHz for optimized spacing of S=35 mm. The on-axis axial ratio (AR) will show the variation of AR at fixed angle (ɵ= 0°) only. To verify this AR at other angles, the off-axis AR is also simulated. The off-axis AR is plotted at discrete frequencies over the band. These ON and OFF axes plots are shown in Fig. 7.

As can be seen from these plots, the antenna beam width varies from 54°-130° for 3 dB axial ratio. The variation of realized gain of the antenna is studied as function of spacing.

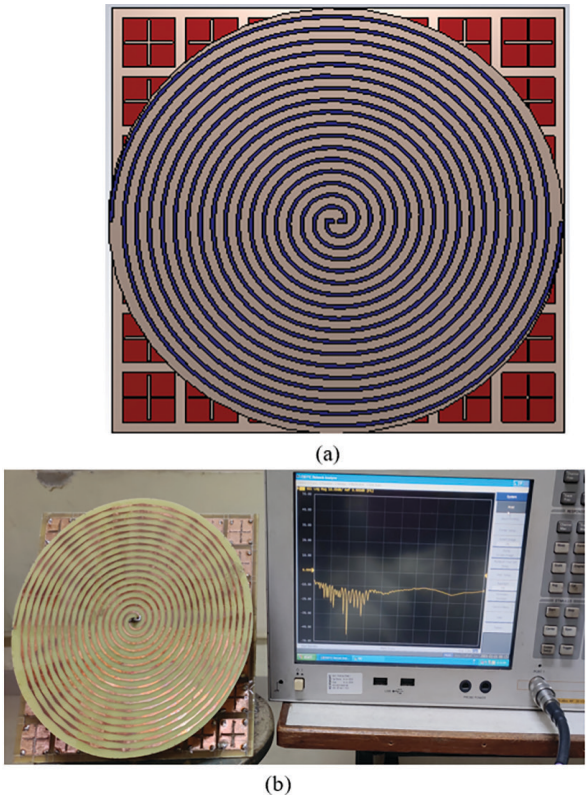

Figure 5. Spiral antenna with metamaterial reflector antenna simulation model; and (b) Realized antenna with return loss measurement setup.

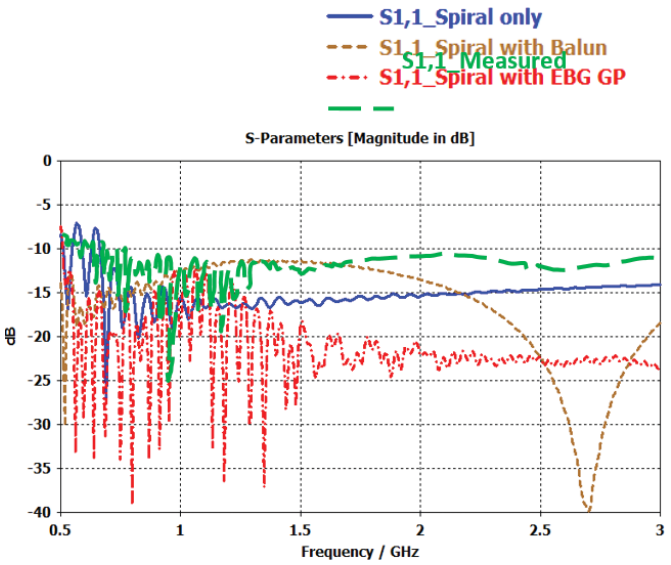

Figure 6. Return loss comparison of spiral antenna for its different stages and measured return loss.

For a spacing variation from 25 mm to 45 mm, 2 dB gain variation is observed. For optimized dimensions, the realized antenna gain varies from 5 dBic to 8.5 dBic over the frequency band. The gain improvement of the order of 1.5 dB to 3.5 dB is achieved compared to spiral antenna without any reflector over the band. This shows the effectiveness of the metamaterial ground plane.

The proposed antenna was evaluated for its radiation patterns in two principal cuts. These radiation patterns cuts are

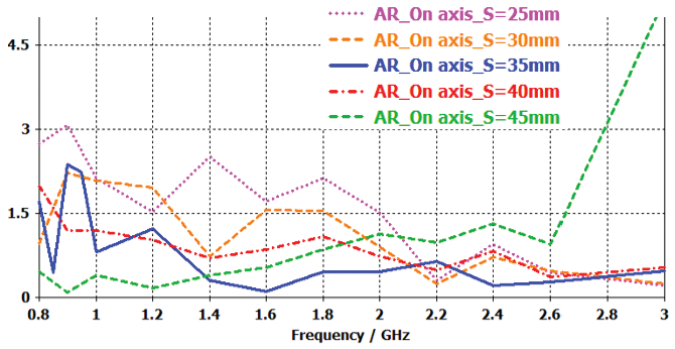

(a)

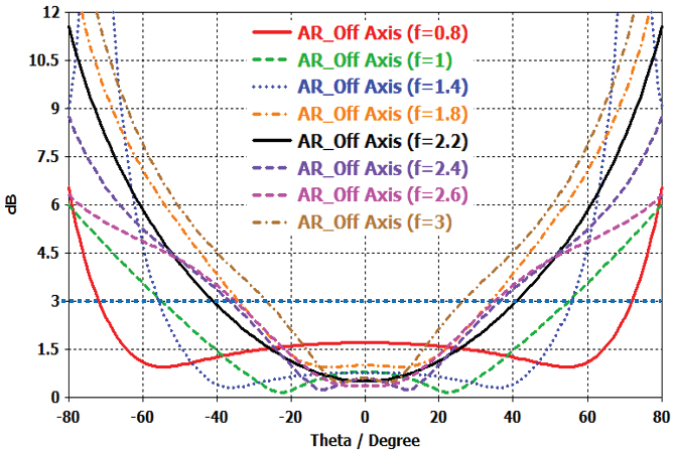

(b)

Figure 8. Axial Ratio (AR) plots of the proposed antenna (a) Boresight (on-axis) as function of spacing (S); and (b) off-axis at discrete frequencies.

at ϕ= 0° and ϕ= 90°. These two radiation patterns cuts provide the beam width variation over the band in two planes. To validate the simulated radiation characteristics of the proposed antenna, the radiation patterns measurement is carried out in an anechoic chamber. The overlay of simulated and measured radiation patterns are shown in Fig. 8.

In measured radiation patterns, a marginal gain improvement of 1 dB to 1.5 dB is observed due to improvement in front to back ratio. This is attributed to unavoidable antenna mounting plate in antenna positioning system of anechoic chamber, behaving as a reflector.

3. PERFORMANCE COMPARISON WITH SIMILAR DESIGNS

The performance of the proposed antenna is compared with similar designs available in literature[9-15]. Mainly these designs are based on metamaterial ground planes. The EBG cells used in these ground planes are derived from mushroom-like EBG cells. Type of radiating element, reflector size, spacing between antenna and reflector (S), impedance, and 3 dB axial ratio bandwidths were the basis for this comparison. This comparison is shown in Table 4.

As evident from this comparison, the only impedance and radiation patterns bandwidths are included by most of the authors. The AR band width being an important parameter for circularly polarized antenna is missing in most of the references.

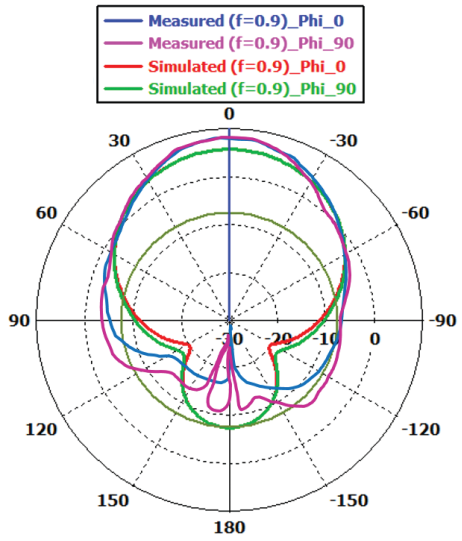

(a)

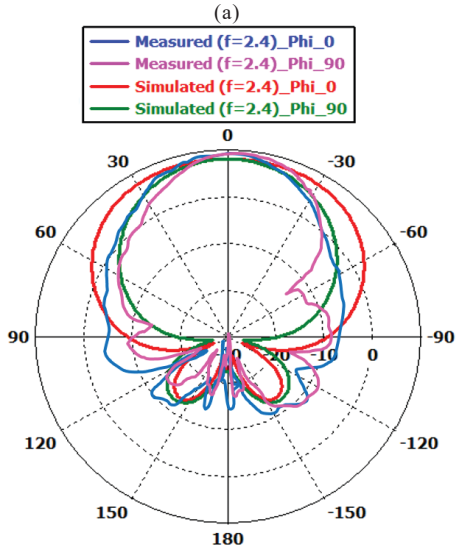

(b)

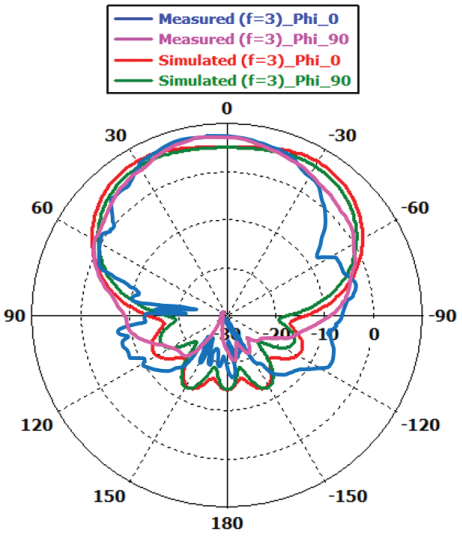

(c)

Figure 8. (a-c) Overlay of simulated and measured radiation patterns in two principal cuts, φ = 0 and φ = 90°.

Table 4. Performance comparisons of proposed antenna with available designs in the literature

Ref.	Radiating element	Reflector Parameters	Radiator to Reflector Spacing	Mid-band freq. (f0) (GHz)	Bandwidth (%)	
					Impedance & Radiation Patterns	3 dB AR
9	Square spiral	Mushroom-like EBG, Size: 2.18 λ x2.18 λ	0.1 λ	6 GHz	-------	11 (Boresight)
10	Archimedean spiral	Mushroom-like EBG, Size: 1.1 λ x1.1 λ	0.02 λ	12 GHz	42	-------
11	Archimedean spiral	Resistively loaded Metallic patches, Size:0.43 λ x0.43 λ	0.006 λ	5.5 GHz	163.6	-------
12	Equiangular spiral	Modified Mushroom-like EBG, Size: 5.5 λ x4 λ	0.06 λ	3 GHz	66.7	-------
13	Equiangular spiral	Mushroom-like EBG, Size: 2.23 λ x2.23 λ	0.07 λ	6.5 GHz	76.9	76.9 (Boresight)
14	Archimedean spiral	Mushroom-like EBG, Size: 0.93 λ x0.93 λ	0.02 λ	15 GHz	66.7	-------
15	Archimedean spiral	DGS, 0.51 λ x0.51 λ	0.05 λ	3.5 GHz	70.0	70.0 (Boresight) 70.0 (Off-axis)
This work	Archimedean spiral	Mushroom-like with quad-via and cross-slots Size: 0.5 λ x0.5 λ	0.09 λ	1.9 GHz	115.8	115.8 (Boresight) 1.8 (Off-axis)

4. CONCLUSION

A novel EBG cell is designed to have better electrical characteristics. The metamaterial ground plane is configured and tested for its electromagnetic band gap properties. This ground plane was used as a reflector for the spiral antenna to utilize its extraordinary properties which are not possible with conventional metallic ground planes. A broadband circularly polarized antenna has been designed, developed and realized for anti-drone applications. The electrical parameters for this antenna are verified by simulation and measurement. The proposed antenna is low-profile antenna compared to its counterpart cavity-backed spiral antenna. This antenna has very less height compared to helical antennas conventionally used in anti-drone technology. The antenna being high gain circularly polarized antenna can be used for Trans-receive roles in the said technology.

REFERENCES

1. Sievenpiper, D.F. High-impedance electromagnetic surfaces. University of California, Los Angeles, 1999. (Ph.D. dissertation).
2. Yang, F. & Rahmat-Samii, Y. Polarization-dependent electromagnetic band gap (PDEBG) structures: designs and applications. *Microwave Opti. Technol. Lett.*, 2004, **41**(6), 439–444.
3. Ahirwar, S.D.; Rao, A.P. & Chakravarthy, M. Design of a high gain low profile dipole antenna using EBG Ground plane as a Reflector. *In* 2nd International Conference on Emerging trends in Engineering (ICETE), Osmania University, India, April 28-30, 2023, AER-223 (Springer), 2023, 845-853.
4. Kahn, K.B. Understanding innovation. Business Horizons, **61**, 2018, pp. 453-460.
5. Straub, J. Unmanned aerial systems: Consideration of the use of force for law enforcement applications. *Technol. in Soc.*, **39**, 2014, 100-109.
6. Seongjoon, P.; Hyeong; Tae K.; Sangmin L; Hyeontae, J. & Hwangnam K. Survey on Anti-Drone system: Components, Design, and challenges. *IEEE Access*, 2020.
7. Svetoslav, Z.; Garo, M. & Roumen, N. Recent innovations in circularly polarized antennas for drone radio communication. C.R. Acad. Bulgarian Sciences Sept., 2020, **73**(9), 1286-1290.
8. Kaiser, J. The Archimedean two-wire spiral antenna. IRE Trans. *Antennas Propag.*, 2019, AP-8(**3)**, 312–323.
9. Nakano, H.; Ikeda, M.; Hitosugi, K.; Yamauchi, J**.** & Hirose, K. A spiral antenna backed by an electromagnetic band-gap material. IEEE Antennas and Propagation Society International Symposium, 22-27 June 2003. doi: 10.1109/APS.2003.1220315.
10. Jodie, M.B. & Magdy I.F. A low-profile archimedean spiral antenna using an EBG ground plane. *IEEE Antennas and Wireless Propag. Lett.*, **3**. doi: 10.1109/LAWP.2004.835753.
11. Schreider, L.; Begaud, X.; Soiron M. & Perpere, B. Design of a broadband archimedean Spiral Antenna above a thin Modified Electromagnetic Band Gap Substrate. *In* 1st European Conference on Antennas and Propagation, EuCAP, 2006. doi: 10.1109/EUCAP.2006.4584969.
12. Zhong, Li; Guangming, W. & Cao, Y. A low-profile equiangular spiral antenna using a novel EBG ground plane. 7th International Symposium on Antennas, Propagation & Amp; EM Theory, 2006. doi: 10.1109/ISAPE.2006.353349.
13. Hisamatsu, N.; Katsuki, K.; Norihiro, K.; Yasushi, I. & Junji, Y. Low-profile equiangular spiral antenna backed by an EBG reflector. *IEEE Transact. Antennas and Propag.*, 2009, **57**(5). doi: 10.1109/TAP.2009.2016697.
14. Sen, Du; Wenqi, Z.; Jiaye, Z. & Rushan, C. Design of a broadband Archimedean spiral antenna above an EBG

ground plane. 2019 International Applied Computational Electromagnetics Society Symposium - China (ACES) Aug. 2019, 8-11.
doi: 10.23919/ACES48530.2019.9060522.

15. Ahirwar, S.D.; Rao, A.P. & Chakravarthy, M. Design of a low profile Archimedean spiral antenna using compact defected ground plane as reflector. *Def. Scie. J.*, 2023, **73**(5), 572-581.
doi:10.14429/dsj.73.5.17751.

CONTRIBUTORS

Mr Sukhdas Ahirwar obtained his M.E. (ECE) in Microwave & Radar Engineering from Osmania University, Hyderabad and working as a Scientist in DRDO-DLRL, Hyderabad. His areas of interest include: Electrically small broadband antennas, broadband HF/VHF/UHF EW antennas and metamaterials.
Contribution in the current research work: He carried out the literature survey of the similar works available. Identified the gaps and conceptualized the design accordingly. Predicted the results by Simulation and validated by measurements.

Dr Amara Prakasa Rao obtained his doctoral degree from National Institute of Technology Warangal, India and working as an Associate Professor at National Institute of Technology, Warangal, India. His areas of interest include: Signal processing, smart antenna systems, and optimization techniques.
Contribution in the current research work: He has supervised the research work, contributed for theoretical correlation with simulation results and organization of the Paper.

Dr M. Chakravarthy obtained PhD from Andhra University, Visakhapatnam. He is working as Scientist 'H' at DRDO-DLRL, Hyderabad. His areas of research include: Indigenous development of variety of state of the art Broadband EW antennas and radomes covering HF to MMW frequency ranges for all three services.
Contribution in the current research work: He has provided overall guidance and support in testing and analysis of results, measurement setup and review of the research paper.